Journal of Radiation Research, Vol. 63, No. 4, 2022, pp. 585–590
https://doi.org/10.1093/jrr/rrac022
Advance Access Publication: 20 May 2022

Double-layer omics analysis of castration- and X-ray-resistant prostate cancer cells

Mototaro Iwanaga[1], Hidemasa Kawamura[1,*], Nobuteru Kubo[1], Tatsuji Mizukami[1], Takahiro Oike[1], Hiro Sato[1], Yoshiyuki Miyazawa[2], Yoshitaka Sekine[2], Reika Kawabata-Iwakawa[3], Masahiko Nishiyama[3,4], Tatsuya Ohno[1] and Takashi Nakano[1]

[1]Department of Radiation Oncology, Gunma University Graduate School of Medicine, 3-39-22 Showa-machi, Maebashi, Gunma, 371-8511, Japan
[2]Department of Urology, Gunma University Graduate School of Medicine, 3-39-22 Showa-machi, Maebashi, Gunma, 371-8511, Japan
[3]Division of Integrated Oncology Research, Gunma University Initiative for Advanced Research, 3-39-22 Showa-machi, Maebashi, Gunma, 371-8511, Japan
[4]Department of Molecular Pharmacology and Oncology, Gunma University Graduate School of Medicine, 3-39-22 Showa-machi, Maebashi, Gunma, 371-8511, Japan
*Corresponding author. 3-39-22 Showa-machi, Maebashi, Gunma, 371-8511, JAPAN, Phone: +81-27-220-8383, Fax: +81-27-220-8397, E-mail: kawa@gunma-u.ac.jp
(Received 28 February 2021; revised 31 January 2022; editorial decision 1 April 2022)

ABSTRACT

Castration-resistant prostate cancer shows resistance to not only androgen deprivation therapy (ADT) but also X-ray therapy. On the other hand, carbon ion beams have a high biological effect and are used for various cancers showing resistance to X-ray therapy. The purposes of this study are to clarify the difference in the sensitivity of Castration-resistant prostate cancer to X-ray and carbon ion beams and to elucidate the mechanism. The androgen-insensitive prostate cancer cell line LNCaP-LA established by culturing the androgen-sensitive prostate cancer cell line LNCaP for 2 years in androgen-free medium was used for this study. First, colony formation assays were performed to investigate its sensitivity to X-ray and carbon ion beams. Next, DNA mutation analysis on 409 cancer-related genes and comprehensive transcriptome analysis (RNA-seq) were performed with a next-generation sequencer. Lethal dose 50 values of X-rays for LNCaP and LNCaP-LA were 1.4 Gy and 2.8 Gy, respectively ($P < 0.01$). The Lethal dose 50 values of carbon ion beams were 0.9 Gy and 0.7 Gy, respectively ($P = 0.09$). On DNA mutation analysis, *AR* mutation was observed specifically in LNCaP-LA. From RNA-seq, 181 genes were identified as differentially expressed genes (DEGs; FDR <0.10, $P < 0.00076$) between LNCaP and LNCaP-LA. Function analysis suggested that cell death was suppressed in LNCaP-LA, and pathway analysis suggested that the NRF2-pathway involved in intracellular oxidative stress prevention was activated in LNCaP-LA. LNCaP-LA showed X-ray resistance compared to LNCaP and sensitivity to carbon ion beams. The *AR* mutation and the NRF2-pathway were suggested as causes of resistance.

Keywords: castration-resistant prostate cancer; X-ray resistance; carbon ion beam; AR; NRF2-pathway

INTRODUCTION

Prostate cancer is one of the most common male cancers and was one of most common causes of men's cancer death in the world. Androgen deprivation therapy (ADT) is often effective because prostate cancer needs androgen to grow. Despite serum testosterone levels being maintained at castrate levels by ADT, progression of prostate cancer may be observed, and prostate cancer can become castration-resistant prostate cancer (CRPC). Although X-ray therapy is sometimes performed for localized CRPC [1], the clinical outcome was poor compared to that for T1-2 not CRPC [2]. Thus, treatment for CRPC needs to be improved. *In vitro* or *in vivo,* CRPC shows resistance to X-rays, and it has been shown that reduction of p53 and increases of *AR* and *MDM2* might be related X-ray resistance in CRPC [3]. However, the mechanism has not been clarified. Carbon ion beams have high dose concentration because of their Bragg Peak. In addition, carbon ion beams have high linear energy transfer (LET) that induces clustered DNA damage leading to a high biological effect [4]. Because of these characteristics, carbon ion beams are effective against X-ray-resistant

tumors [5]. However, little is known about the biological sensitivity of carbon ion beams for CRPC and the clinical usefulness of carbon ion therapy for CRPC has not yet been clarified. Therefore, the purpose of this study was to clarify the difference in sensitivity of CRPC to X-ray and carbon ion beams and to investigate the mechanism of the difference.

MATERIALS AND METHODS

Cell lines and culture

LNCaP and LNCaP-LA cell lines were provided in our institution. These cell lines were established from human prostate cancer. Because LNCaP has androgen dependency, LNCaP do not survive in medium containing charcoal-stripped fetal bovine serum (CSFBS) only. To establish androgen independent cell lines, LNCaP cells were cultured in medium containing 9% CFFBS and 1% FBS for 2 weeks. Then, CSFFBS was gradually increased and FBS was gradually decreased. Finally, cells were cultured in medium containing 10% CSFBS only. Cells that survived were harvested and expanded in the androgen deficient culture medium for more than 3 months were designated LNCaP-LA.

LNCaP was cultured in RPMI-1640 (Sigma-Aldrich Co.) supplemented with 10% FBS, 5 ml penicillin–streptomycin (× 100) and 5 ml pyruvate (100 mM). LNCaP-LA was cultured in RPMI-1640, no phenol red, supplemented with 10% CSFFBS and 5 ml of penicillin–streptomycin (× 100) and 5 ml pyruvate (100 mM). Cells were cultured at 37°C under 5% CO_2.

Cell irradiation

X-ray irradiation was performed at our institution using a Faxitron RX-650 (100 kVp, 1.14 Gy/min, Faxitron Bioptics). Carbon ion irradiation was performed in our institution using 290 MeV/nucleon at the center of a 3.5 cm spread-out Bragg peak [6].

Colony formation assay

Cells were seeded in 25-cm^2 dishes with RPMI-1640 (Sigma-Aldrich Co) 10% fetal bovine serum, penicillin–streptomycin and pyruvate. These cells were cultured for one day and irradiated by 1–4 Gy (X-ray) or 0.5–2 Gy (carbon ion beam). After irradiation, cells were incubated for 2 weeks. The colonies were fixed with methanol and stained with crystal violet. Colonies containing more than 50 cells were considered survivors. Experiments were done in triplicate. Curve fitting for the surviving fraction was done using a linear quadratic model. Statistical differences were evaluated using Student's *t*-test, and $P < 0.05$ was considered significant.

Genome analysis

DNA was isolated from LNCaP and LNCaP-LA using QIAamp DNA Blood Midi/Maxi (Qiagen, Inc., Valencia, CA). The Ion AmpliSeq Comprehensive Cancer Panel was used to sequence hotspot regions in 409 frequently mutated tumor suppressor genes and oncogenes in cooperation with Sapporo Medical University as a Genome Project supported by the Ministry of Education, Culture, Sports and Technology (Fig. S1 and Table S1). Average read depth in analyzable target region was 287.5 and percentage of analyzable target base with at least 20 reads was 96.88%.

In order to eliminate erroneous base calling, several filtering steps were used for final generated variant calling. The first filter was set at an average depth of total coverage of >30, and synonymous was excluded. The second filter satisfied the following conditions: SIFT <0.05, PolyPhen 0.05–1.0 and Grantham 25–215. The third filter was variant frequency LNCaP <1% and LNCaP-LA >10% Next, ontological analysis was performed. These variants were confirmed by Sanger's sequencing.

Whole transcriptome sequence

Total RNA was extracted using a NucleoSpin RNA kit (TaKaRa Bio, Shiga, Japan) according to the manufacturer's protocol. RNA quality was assessed using an Agilent Bioanalyzer (Agilent Technologies, Santa Clara, CA), and high-quality RNAs (RNA integrity numbers >9.0) were used for RNA-seq. One microgram of total RNA was used to generate sequencing libraries using the TruSeq RNA Sample Prep Kit (Illumina®, San Diego, CA, USA) following the manufacturer's instructions. Libraries were subjected to paired-end sequencing of 43-bp reads using a NextSeq500 System (Illumina) with a NextSeq500 High Output Kit (Illumina). The reads were aligned to the UCSC reference human genome 19 (hg19) using a Spliced Transcripts Alignment to a reference (STAR) software v2.3.1 (DNASTAR, Inc., Madison, WI, USA). The Integrative Genomics Viewer (IGV) was used for validation of the variants identified by the Ion AmpliSeq Comprehensive Cancer Panel sequencing [7]. TCC-DESeq was used to normalize and identify differentially expressed genes (DEGs) [8, 9]. Pathway analysis was conducted using IPA software (QIAGEN, Ingenuity Systems, www.ingenuity.com).

RESULTS

Colony formation assay

Figure 1 and Fig. S2 show the effects of X-ray and carbon ion beams on the colony formation assay. In X-ray irradiation, the doses required to kill 50% of the population (LD50) were 1.4 Gy for LNCaP and 2.8 Gy for LNCaP-LA ($P < 0.01$). In carbon ion irradiation, LD50 values were 0.9 Gy for LNCaP and 0.7 Gy for LNCaP-LA ($P = 0.09$). At LD50, the relative biological effectiveness (RBE, LD50 in X-ray/LD50 carbon ion beam) of LNCaP was 1.92 and the RBE of LNCaP-LA was 3.96.

Genome analysis

Two single-nucleotide variants (SNVs, *AR*, *PRKDC*) and two insertion or deletion (INDEL, *KMT 2 D*, *PTEN*) were detected as specific mutations in LNCaP-LA by the Ion AmpliSeq Comprehensive Cancer Panel. Among them, *AR* and *PRKDC* gene mutations were confirmed as a result of these gene mutations by Sanger's method (Fig. S3).

Whole transcriptome analysis

Among four mutations identified in the genome analysis, expression of mutant alleles in *AR* and *PRKDC* were also validated (variant allele frequencies = 48% and 20%, respectively) by RNA-seq.

One hundred eighty-one genes were identified as significantly ($q < 0.1$) DEGs (Fig. 2). Among them, 82 DEGs were up-regulated

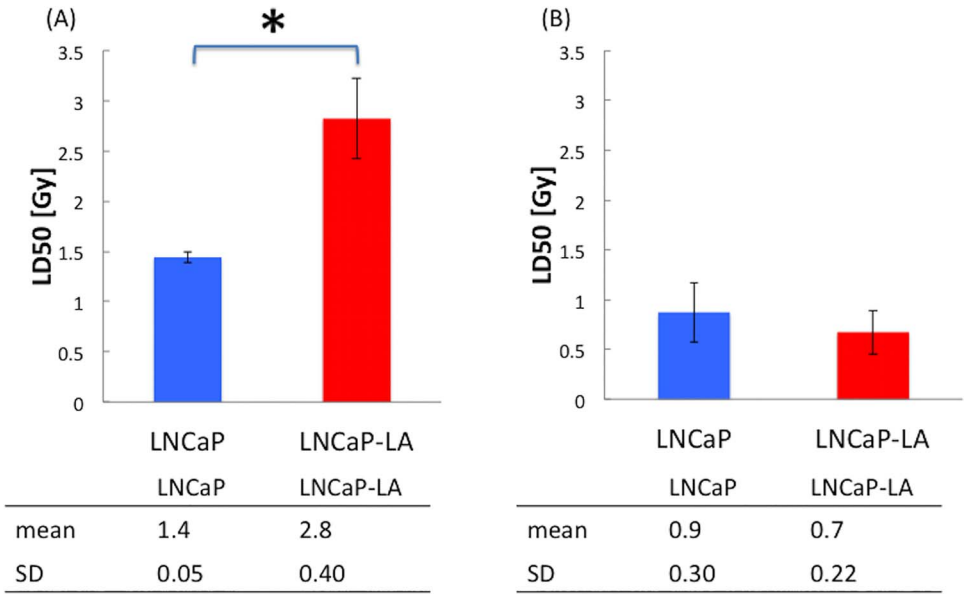

	LNCaP	LNCaP-LA
mean	1.4	2.8
SD	0.05	0.40

	LNCaP	LNCaP-LA
mean	0.9	0.7
SD	0.30	0.22

Fig. 1. Result of colony formation assay. (A) LD50 of LNCaP and LNCaP-LA with X-ray irradiation. (B) LD50 of LNCaP and LNCaP-LA with Carbon ion beam irradiation. $^{*}P < 0.01$.

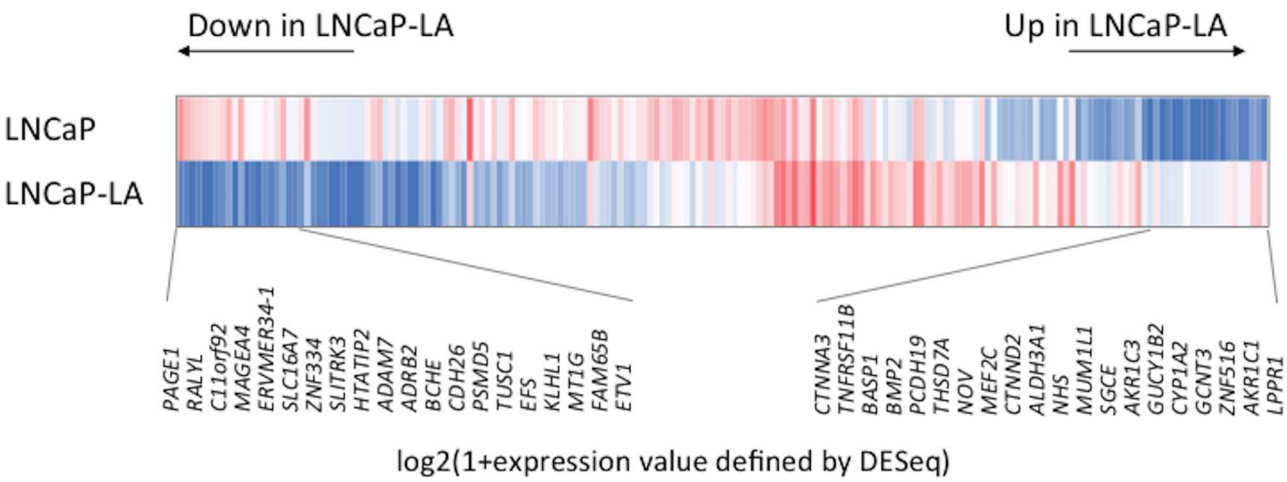

Fig. 2. Heatmap of 181 genes modulated between LNCaP-LA and LNCaP. The heatmap shows gene expression values for LNCaP and LNCaP-LA. Red represents higher expression and blue represents lower expression.

and 99 DEGs were down-regulated in LNCaP-LA compared to LNCaP (Table S2).

To identify the significantly enriched pathway and predict the functional effects of the LNCaP-LA, we performed the 'Core Analysis' for the 181 DEGs by using the IPA. Table 1 shows Top 20 Pathway of -log (*P*-value). Z-score in NF-E2-related factor 2 (NRF 2)-mediated oxidative stress response pathway was the highest in this study.

The results of functional analysis are shown in Table 2. The activated functions (Z-score > 2) in LNCaP-LA compared to LNCaP were category of generation of cells and category of development of neurons. The inactivated functions (Z-score < −2) were category of apoptosis, category of organismal death and category of necrosis. In addition, the activation Z-score in category of oxidative stress was −1.969.

DISCUSSION

LNCaP-LA showed more resistance to X-ray than LNCaP, but there was no significant difference in sensitivity to the carbon ion beam between LNCaP-LA and LNCaP. In the present study of genome analysis showed that *AR* was considered a target gene related to X-ray resistance. Moreover, the NRF2 pathway was significantly activated in LNCaP-LA compared to LNCaP. From the functional analysis, LNCaP-LA showed increases in categories of cell proliferation

Table 1. Top 20 pathway [−log(*P*-value)]

Ingenuity Canonical Pathways	-log(*P*-value)	Ratio	z-score	Molecules
Glutathione Biosynthesis	3.70E+00	6.67E-01	NaN	GCLC, GCLM
Xenobiotic Metabolism Signaling	3.38E+00	3.31E-02	NaN	MAPK13, UGT2B28, ALDH3A1,
cAMP-mediated signaling	3.34E+00	3.65E-02	0	GNAI1, ADRB2, CNGB3, PDE4D, ADRA2A, NPR3, PDE10A, DUSP4
Cardiomyocyte Differentiation Via BMP Receptors	3.25E+00	1.50E-01	NaN	BMP2, MEF2C, BMPR1B
Serotonin Degradation	2.65E+00	5.97E-02	NaN	UGT2B17, UGT2B28, ALDH3A1, DHRS2
NRF2-mediated Oxidative Stress Response	2.43E+00	3.33E-02	2	GCLC, DNAJC15, GCLM, FTH1, HMOX1, ENC1
Bile Acid Biosynthesis, Neutral Pathway	2.31E+00	1.54E-01	NaN	AKR1C3, AKR1C1/AKR1C2
Relaxin Signaling	2.29E+00	3.70E-02	NaN	GNAI1, GNB4, GUCY1B3, PDE4D, PDE10A
G-Protein Coupled Receptor Signaling	2.28E+00	2.73E-02	NaN	GNAI1, ADRB2, PDE4D, ADRA2A, NPR3, PDE10A, DUSP4
Bladder Cancer Signaling	2.24E+00	4.60E-02	NaN	FGFR3, DAPK1, FGF13, MMP16
γ-glutamyl Cycle	2.18E+00	1.33E-01	NaN	GCLC, GCLM
Methylglyoxal Degradation III	2.13E+00	1.25E-01	NaN	AKR1C3, AKR1C1/AKR1C2
Amyloid Processing	2.07E+00	5.88E-02	NaN	CAPN5, BACE2, MAPK13
Nicotine Degradation III	2.01E+00	5.56E-02	NaN	CYP1A2, UGT2B17, UGT2B28
Cardiac Hypertrophy Signaling	1.99E+00	2.69E-02	−0.447	GNAI1, ADRB2, GNB4, MAPK13, ADRA2A, MEF2C
Melatonin Degradation I	1.94E+00	5.26E-02	NaN	CYP1A2, UGT2B17, UGT2B28
Corticotropin Releasing Hormone Signaling	1.88E+00	3.60E-02	−1	GNAI1, GUCY1B3, MAPK13, MEF2C
Role of NFAT in Regulation of the Immune Response	1.87E+00	2.92E-02	NaN	GNAI1, GNB4, HLA-DMB, BLNK, MEF2C
Endothelin-1 Signaling	1.86E+00	2.91E-02	−0.447	GNAI1, PLA2G16, GUCY1B3, MAPK13, HMOX1
Superpathway of Melatonin Degradation	1.84E+00	4.84E-02	NaN	CYP1A2, UGT2B17, UGT2B28

Table 2. Top 5 increased and decreased activation z-score in LNCaP-LA

Diseases or Functions Annotation	*P*-Value	Activation z-score
Generation of cells	5.86E-03	3.06
Development of neurons	4.96E-03	2.13
Migration of carcinoma cell lines	9.91E-04	1.97
Differentiation of neurons	5.66E-03	1.67
Proliferation of prostate cancer cell lines	1.16E-05	1.65
Cell death	5.86E-04	−1.80
Oxidative stress	1.89E-03	−1.97
Apoptosis	2.38E-04	−2.01
Organismal death	1.91E-06	−2.31
Necrosis	2.14E-04	−2.39

and inhibition of cell death such as apoptosis. The NRF2 pathway is considered as a cause of X-ray resistance.

LNCaP-LA as an *in vitro* model of CRPC showed resistance to X-ray, but there was no significant difference in sensitivity to the carbon ion beam compared to LNCaP as androgen dependent prostate cancer cell line. LNCaP-LA was used as an *in vitro* model of CRPC on several reports [10–12]. LNCaP-LA was established with not chemotherapy but hormone deprivation. Clinically, a lot of patients with prostate cancer receive not chemotherapy but ADT as the first-line systemic therapy. An androgen-independent prostate cancer cell line, C4–2,

established from LNCaP showed more X-ray resistance than LNCaP [13]. In the present study, LNCaP-LA showed more X-ray resistance than LNCaP. These results indicated that androgen resistant prostate cancers tend to be resistant to X-ray. However, the response and mechanisms of carbon ion beams in CRPC have not been clarified. In the present study, RBE values of carbon ion beam for LNCaP and LNCaP-LA at LD50 were 1.92 and 3.96, respectively. This result showed that LNCaP-LA was X-ray resistant compared to LNCaP at LD50, and carbon ion beams showed the similar cell killing effect for LNCaP-LA and LNCaP. Thus, it appears that carbon ion beams are effective for CRPC showing X-ray resistance.

LNCaP-LA is a cell line isolated and established from LNCaP, and it seems that DNA mutations between the two cell lines seems to be deeply related to acquisition of castration resistance and X-ray resistance. From the genome analysis, *AR* mutation was considered a target gene mutation. The mutation of *AR* was identified at W742C in the ligand binding domain (LBD), which was confirmed by RNA-sequencing. Mutations in the LBD usually result in lack of specificity of the AR to other hormones [14]. *AR* mutation plays a central role in prostate cancer acquiring castration resistance [9]. Our results showed that *AR* mutation was observed specifically in LNCaP-LA. Further, Bartek *et al.* reported that the AR is activated by irradiation and promotes transcription of many DNA repair genes, including *PRKDC*. Thus, prostate cancer acquires X-ray resistance [15]. *AR* mutation was considered causes of X-ray resistance, because LNCaP-LA showed X-ray resistant in the present study. The results of RNA sequencing identified 181 DEGs as genes showing significant expression variation in LNCaP-LA relative to LNCaP (Table S2). The canonical pathway analysis showed that Z-score in NRF2 pathway is the highest. Z-score is statistical measure of correlation between relationship direction and gene expression. We focused on NRF2 pathway. NRF2 pathway is involved in oxidative stress defense. Reactive oxygen species (ROS) are generated by exogenous sources such as ionizing radiation. Under non-oxidative stress conditions, NRF2 binds to KEAP1 in the cytoplasm. In contrast, under oxidative stress conditions, KEAP1 releases NRF2. Then, NRF2 binds to androgen-responsive elements to activate transcription of oxidant enzyme genes, HO-1 and FTH-1, etc. The NRF2 pathway is considered a main defense mechanism of normal cells against oxidative stress [16]. On the other hand, hyperactivation of the NRF2 pathway in cancer cells contributes to resistance to chemotherapy and radiotherapy [17]. In the present study, gene expressions of GCLM, GCLC, HO-1 and FTH 1, which are included in the NRF2 pathway, were increased. GCLM and GCLC are involved in glutathione (GSH) synthesis. GSH is also involved in redox signaling, is vital in detoxification of xenobiotics, and modulates cell proliferation, apoptosis, immune function and fibrogenesis [18]. Functions of HO-1 are protection against oxidative injury, regulation of apoptosis and modulation of inflammation, as well as contributing to angiogenesis [19]. In the present study, activated NRF2 pathway may cause X-ray resistance of LNCaP-LA.

In the present study, LNCaP-LA showed more suppression of apoptosis, organismal death and necrosis than LNCaP (Table 2). In addition, LNCaP-LA showed increased generation of cells and development of neurons than LNCaP. Neuroendocrine differentiation in prostate cancer is a phenotypic change. ADT can induce this change, and the neuroendocrine differentiation is correlated with poor survival in CRPC patient [20]. In this study, category of development of neurons increased in LNCaP-LA. This change may lead to X-ray resistance. Various reports have already shown the suppression of apoptosis and necrosis contributing to the X-ray resistance of cancer [21]. In the study of a prostate cancer cell line, suppressing apoptosis-suppressing factor could overcome X-ray resistance [22]. Furthermore, the activation Z-score of oxidative stress was −1.969. That result showed that LNCaP-LA was more resistant to oxidative stress than LNCaP.

Because X-ray is low LET, it induces mainly an indirect effect on DNA; the X-rays hit water molecules, whereby free radicals such as ROS are produced and damage to DNA. The NRF2 pathway is an antioxidant defensive system. LNCaP-LA showed X-ray resistance because LNCaP-LA had hyperactivation of the NRF2 pathway. In contrast, because the carbon ion beam is high LET, the carbon ion beam hits the DNA directly and cause severe DNA damage. Because the effect does not depend on free radicals, the NRF2 pathway may not play a role in cell survival in carbon ion irradiation. This is the reason why there was no significant difference in sensitivity to carbon ion beam irradiation between LNCaP-LA and LNCaP.

There are several limitations in our study. First, it was *in vitro* research. This result is not verified in vivo. Second, DNA analysis was not performed on the whole genome. Therefore, DNA mutations other than the 409 frequently mutated tumor suppressor genes and oncogenes in genome analysis were not analyzed. Third, we do not verify that NRF2 Pathway and *AR* gene are related to X-ray resistance in LNCaP-LA with other methods, for instance, that suppress the pathway and the gene.

In conclusion, the CRPC cell line showed X-ray resistance compared with an androgen-dependent prostate cancer cell line, but carbon ion beams were effective both in androgen-dependent prostate cancer cell and CRPC cell lines. *AR* mutation and activation of the NRF2 pathway in the CRPC cell line may be considered causes of X-ray resistance. It is necessary to clarify how that gene mutation and this pathway play a role in CRPC.

SUPPLEMENTARY MATERIAL

Supplementary material is available at *RADRES Journal* online.

CONFLICT OF INTEREST

The authors declare no conflicts of interest associated with this manuscript.

REFERENCES

1. Akimoto T, Kitamoto Y, Saito J et al. External beam radiotherapy for clinically node-negative, localized hormone-refractory prostate cancer: impact of pretreatment PSA value on radiotherapeutic outcomes. *Int J Radiat Oncol Biol Phys* 2004;59:372–9.
2. Zietman AL, Chung CS, Coen JJ et al. 10-year outcome for men with localized prostate cancer treated with external radiation therapy: results of a cohort study. *J Urol* 2004;171:210–4.

3. Wu CT, Chen WC, Liao SK et al. The radiation response of hormone-resistant prostate cancer induced by long-term hormone therapy. *Endocr Relat Cancer* 2007;14:633–43.
4. Ohno T. Particle radiotherapy with carbon ion beams. *EPMA J* 2013;9:1–7.
5. Ebner DK, Kamada T. The emerging role of carbon-ion radiotherapy. *Front Oncol* 2016;6:6–11.
6. Ohno T, Kanai T, Yamada S et al. Carbon ion radiotherapy at our institution: new facility set-up. *Cancers* 2011;3:4046–60.
7. Robinson JT, Thorvaldsdottir H, Winckler W et al. Integrative genomics viewer. *Nat Biotechnol* 2011;29:24–6.
8. Sun Q, Muckatira S, Yuan L et al. Image-level and group-level models for Drosophila gene expression pattern annotation. *BMC Bioinform* 2013;14:1–13.
9. Muramatsu K, Matsui H, Sekine Y et al. Amdrogen receptor caactivator p120 subtype beta is highly expressed in prostate cancer. *Prostate Int* 2013;1:10–5.
10. Miyazawa Y, Sekine Y, Kato H et al. Simvastatin up-regulates annexin A10 that can inhibit the proliferation, migration, and invasion in androgen-independent human prostate cancer cells. *Prostate* 2017;77:337–49.
11. Sekine Y, Nakayama H, Miyazawa Y et al. Simvastatin in combination with meclofenamic acid migration of human prostate cancer PC-3 via an AKR1C3 mechanism. *Oncol Lett* 2018;15:3167–72.
12. Anders S, Huber W. Differential expression analysis for sequence count data. *Genome Biol* 2010;11:1–12.
13. Xie BX, Zhang H, Yu L et al. The radiation response of androgen-refractory prostate cancer cell line C4-2 derived from androgen-sensitive cell line LNCaP. *Asian J Androl* 2010;12:405–14.
14. Eisermann K, Wang D, Jing Y et al. Androgen receptor gene mutation, rearrangement, polymorphism. *Transl Androl Urol* 2013;2:137–47.
15. Bartek J, Mistrik M, Bartkova J. Androgen receptor signaling fuels DNA repair and radioresistance in prostate cancer. *Cancer Discov* 2013;3:1222–4.
16. Kim J, Keum YS. *NRF2, a Key Regulator of Antioxidants with Two Faces towards Cancer*. Longev: Oxid. Med. Cell, 2016.
17. Leinonen HM, Kansanen E, Polonen P et al. Dysregulation of the Keap1–Nrf2 pathway in cancer. *Biochem Soc Trans* 2015;43:645–9.
18. Lu SC. Glutathione Synthesis. *Biochim Biophys Acta* 2013;1830:3143–53.
19. Loboda A, Damulewicz M, Pyza E et al. Role of Nrf2 / HO-1 system in development, oxidative stress response and diseases : an evolutionarily conserved mechanism. *Cell Mol Life Sci* 2016;73:3221–47.
20. Hu CD, Choo R, Huang J. Neuroendocrine differentiation in prostate cancer: a mechanism of radioresistance and treatment failure. *Front Oncol* 2015;5:1–10.
21. Janikova M, Skarda J. Differentiation pathways in carcinogenesis and in chemo- and radioresistance. *Neoplasma* 2012;59:6–17.
22. Han Y, Wang L, Yao QP et al. Nuclear envelope proteins Nesprin2 and LaminA regulate proliferation and apoptosis of vascular endothelial cells in response to shear stress. *Biochim Biophys Acta* 2015;1853:1165–73.